

Visualization of spin waves during switching simulation (DF-01)

P. B. Visscher, O. Traistaru, D. M. Apalkov, and Xuebing Feng
*Department of Physics and MINT Center, University of Alabama,
Tuscaloosa, AL 35487-0324*

We discuss "spin-wave switching", in which switching is triggered by a spin wave instability rather than a geometric instability mode such as buckling or curling, or end nucleation. This type of switching was first reported in a simulation by Safonov and Bertram. We examine the mechanism of spin-wave switching using several visualization methods, and introduce a new method of displaying the spin-wave spectrum. We construct a 3D "k-space window" in which the coordinates are the wavevector components k_x , k_y and k_z . At each allowed k-vector in this window we display only the parts of the magnetization attributable to this k-vector. Initially we see magnetization only at $\mathbf{k}=0$, and we can visually follow the exponential growth of the unstable Fourier components at the onset of instability.

I. INTRODUCTION

There has been much recent interest in high-speed (nanosecond and sub-nanosecond) switching in magnetic materials^{1,2,3,4}, partly motivated by the fact that switching speeds in magnetic recording have reached the point where dynamical effects are important. It is no longer sufficient to predict "the material will switch if a reverse field larger than the coercivity is applied", rather we need to understand the switching dynamics. Several mechanisms of switching are fairly well understood. Some of these can be understood without using dynamics, in a quasi-static model of a grain or particle as a grid of computational cells in which each cell's magnetization settles into a local minimum of the Stoner-Wohlfarth energy at each time step – this is valid if the Landau-Lifshitz damping time scale is short compared to the time scale of external field changes. Switching mechanisms that can be modeled with such quasistatic micromagnetic programs include curling and buckling⁵ as well as end-nucleation followed by domain wall motion. However, switching scenarios have been found that do not seem to be describable in these terms. In particular, Safonov and Bertram have described a model in which switching seems to occur through a spin wave instability⁶. We will describe a minimal Safonov-Bertram model (the simplest model that is known to exhibit this "spin wave switching") in Section II. We divide the switching process into a nearly-coherent phase in which the magnetization swings far from the initial direction (but coherently in a closed Stoner-Wohlfarth orbit, which can't be considered switching because of its periodicity) and a coherence-breakup phase in which spin waves appear. We introduce in Section III a new spin-wave visualiza-

tion technique, and use it to show the growth of spin waves in the breakup phase of switching. Together, this gives a fairly complete heuristic picture of how spin-wave switching takes place, which may be used to predict the appearance of this switching mode in more realistic models.

II. SAFONOV-BERTRAM MODEL OF SWITCHING

Safonov and Bertram⁶ have described a model in which spin-wave switching occurs. It consists of a cubic system of $N \times N \times N$ computational cells (they used $N = 2$) in a uniaxially anisotropic medium. Safonov and Bertram considered a finite bounded system; however, since we want to focus on a homogeneous (rather than surface- or shape-induced) switching mechanism, we minimize the effects of the boundaries here by using periodic boundary conditions. (Work is ongoing on the case of a rectangular bounded system.)

The magnetization dynamics is conventionally described using the Landau-Lifshitz (LL) equation for the time evolution of the magnetization \mathbf{M} of a computational cell⁷

$$\frac{d\mathbf{M}}{dt} = -\gamma\mathbf{M} \times \mathbf{H} - \frac{\alpha\gamma}{M_s}\mathbf{M} \times (\mathbf{M} \times \mathbf{H}) \quad (1)$$

The constant $\gamma = 17.6$ (kOe ns)⁻¹ is the gyromagnetic ratio, and α is the LL damping coefficient. The total magnetic field \mathbf{H} consists of an external field, an exchange field, an anisotropy field, the magnetostatic fields of other cells, and a random thermal field whose variance is proportional to temperature. Following Safonov and Bertram⁶, we have simplified the model by initially omitting the magnetostatic and random fields, and the damping constant α . The justification for the latter is that although the damping is important at long times for dissipating spin wave energy (without it, the magnetization never completely reverses⁶ because the system can't get rid of the spin wave energy), until after the breakup phase the effects of damping and random fields are negligible. Thus our total field is

$$\mathbf{H}(\mathbf{r}) = \mathbf{H}^{\text{ext}} + \sum_{\delta} J\mathbf{M}(\mathbf{r} + \delta) + \frac{H_K}{M_s}(\mathbf{M}(\mathbf{r}) \cdot \hat{\mathbf{e}})\hat{\mathbf{e}} \quad (2)$$

where J is the exchange integral, each cell is labeled by its center \mathbf{r} , $\mathbf{r}+\delta$ is one of the six nearest neighbors, $\hat{\mathbf{e}}$ is a unit vector along the easy axis (taken to be the z axis in

this paper), and H_K is the anisotropy field. Although of course our results depend only on dimensionless ratios, for concreteness we have used material constants similar to those of Fe: $4\pi M_s = 20\text{Koe}$ and exchange constant $A = \mu_0 J M_s^2 a^2 = 1.3 \times 10^{-11}\text{J/m}^3$. Choosing the dimensionless exchange parameter (Eq. 2) $J = 0.05$ gives cell size $a = 8.2\text{ nm}$.

In the context of this model, we will now construct a minimal switching scenario. We assume the external field is initially along the $+z$ direction, and reverses to point along $-z$. If the system is initially coherent [$\mathbf{M}(\mathbf{r})$ is independent of \mathbf{r}] it will remain so. Safonov and Bertram broke this coherence by tilting each initial $\mathbf{M}(\mathbf{r})$ randomly; here we have chosen the initial configuration from an equilibrium ensemble generated by stochastic simulation⁹ at a small finite temperature and large external field along z , such that the variance of the tilt angle $\langle \theta^2 \rangle^{1/2} = 0.0008$ radians. If the field is exactly along $-z$, however, we find that the system still does not switch (in the absence of damping). Thus (again following ref.⁶) we tilt the external field by a small angle, by adding a transverse component $H_x^{\text{ext}} = 0.05H_K$. With a positive $H_z^{\text{ext}} = H_K$, for example, we expect that if \mathbf{M} starts out exactly vertical (no random tilt), it will precess around the nearly-vertical external field in a cone whose angle is just a few degrees. The projection of this orbit is shown in Fig. 1a, as the smallest circle, near the origin.

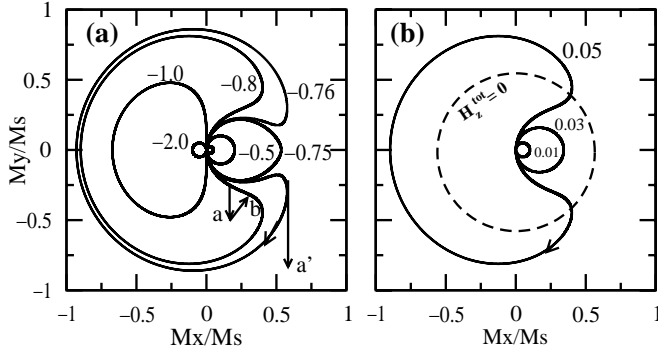


FIG. 1. Orbits of the magnetization, projected onto the $M_x - M_y$ plane, (a) for fixed $H_x^{\text{ext}} = 0.05H_K$ and various values of the vertical component H_z^{ext} . Curves are labeled by H_z^{ext}/H_K , except for the smallest circle, for which this is 1.0. A uniform (Stoner-Wohlfarth) system is assumed. (b) for fixed $H_z^{\text{ext}} = -0.8$, labeled by H_x^{ext}/H_K . Points with $H_z^{\text{ext}} = 0$ lie on the dashed circle.

For a large reverse field, the precession axis cuts the sphere on which \mathbf{M} moves just to the left of the origin, and we get the orbit labeled "-2.0". What may be initially surprising is that there are intermediate values, especially near $H_z^{\text{ext}}/H_K = -1$ for which the precession orbit is very large. One can think of this as because the z component of the total field near the north pole ($M_x = M_y = 0$),

$$H_z^{\text{tot}} = H_z^{\text{ext}} + H_K \frac{M_z}{M_s} \simeq H_z^{\text{ext}} + H_K \quad (3)$$

becomes small, so the transverse component H_x^{ext} dominates, the field makes a large angle with the initial \mathbf{M} , and the precession "circle" is large. To understand the distortion of the circle, however, it is best to think of the velocity $d\mathbf{M}/dt$ along the orbit (from Eq. 1) as having terms proportional to $\mathbf{M} \times \mathbf{H}_x$ (which is labeled 'a' and points down in Fig. 1) and $\mathbf{M} \times \mathbf{H}_z$ ('b', azimuthal in Fig. 1). Initially the latter is zero and there is only downward displacement; as the azimuthal velocity grows, the orbit swings in a counterclockwise direction. For $H_z^{\text{ext}}/H_K = -0.75$, the azimuthal velocity is sufficient to close the orbit counterclockwise before H_z^{tot} (and with it the azimuthal velocity) shrinks to zero, whereas for $H_z^{\text{ext}}/H_K = -0.76$, the azimuthal velocity changes sign (at the point a' where the downward velocity is indicated). In Fig. 1b, we show the orbits for fixed H_z^{ext} , labeling curves with the value of the transverse H_x^{ext}/H_K . Any orbit with a large enough downward velocity (*i.e.*, H_x^{ext}) to cross the dashed $H_z^{\text{tot}} = 0$ circle will turn around and close clockwise.

Even though the orbits in Fig. 1 precess very far from the vertical axis, they do not describe switching because they are closed orbits; energy is conserved. To get switching we must use the slightly noisy initial condition described above. We then get the orbits shown in Fig. 2, in which each of the 64 values of $\mathbf{M}(\mathbf{r})$ is shown as a dot. Initially (near the center of the figure) the system is nearly coherent so the 64 dots at each time form a tight cluster, which spreads with time at an increasing rate, indicating an instability. In the next section, we will try to gain some insight into the nature of this instability.

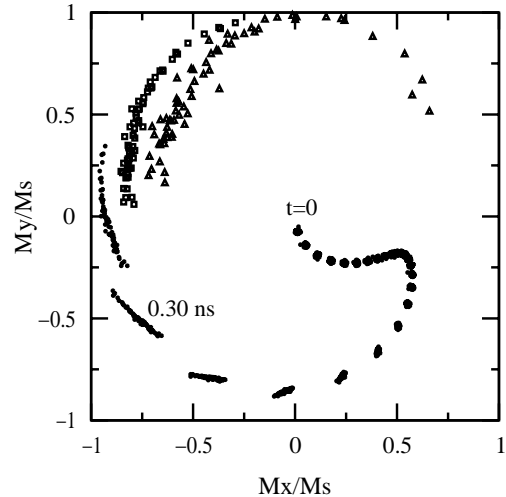


FIG. 2. The orbit with $H_z^{\text{ext}}/H_K = -0.76$ (shown for a coherent system in Fig.1) in a $4 \times 4 \times 4$ system with exchange interactions in which spin waves are possible. Each $\mathbf{M}(\mathbf{r}, t)$ is shown as a filled circle, except at the last two times, $t = 0.3250\text{ ns}$ (squares) and $t = 0.3375\text{ ns}$ (triangles).

III. SPIN-WAVE VISUALIZATION

In a spin wave mode of this system, the $\mathbf{M}(\mathbf{r})$'s precess in a cone about the z axis with time-varying phase angle $\mathbf{k} \cdot \mathbf{r} - \omega t$. We may extract the amplitude of the \mathbf{k}^{th} mode by the Fourier transform⁸

$$\mathbf{M}(\mathbf{k}) = \frac{1}{N^3} \sum_{\mathbf{r}} \mathbf{M}(\mathbf{r}) e^{-i\mathbf{k} \cdot \mathbf{r}} \quad (4)$$

We can then write $\mathbf{M}(\mathbf{r})$ itself as a sum of "spin wave" contributions:

$$\mathbf{M}(\mathbf{r}) = \sum_{\text{pairs}} [\mathbf{M}(\mathbf{k}) e^{i\mathbf{k} \cdot \mathbf{r}} + \mathbf{M}(\mathbf{k})^* e^{-i\mathbf{k} \cdot \mathbf{r}}] \quad (5)$$

where we use a sum over $(\mathbf{k}, -\mathbf{k})$ pairs (except that we omit the second term for $\mathbf{k} = \mathbf{0}$) in order to show explicitly that the result is real, since $\mathbf{M}(\mathbf{k})^* = \mathbf{M}(-\mathbf{k})$. We have implemented a visualization scheme in which we display each term of Eq. 5 at the appropriate point \mathbf{k} in a "k-space window". The vectors $[\mathbf{M}(\mathbf{k}) e^{i\mathbf{k} \cdot \mathbf{r}} + \mathbf{M}(\mathbf{k})^* e^{-i\mathbf{k} \cdot \mathbf{r}}]$ represent the amplitudes of this spin wave at the N^3 points \mathbf{r} . Fortunately there are at most N different values of $\mathbf{k} \cdot \mathbf{r}$, and we display dots at each of these vector positions (relative to the base point \mathbf{k}). We connect the dots by lines – in the limit $N \rightarrow \infty$, this will be an ellipse; in the present case ($N = 4$) it is a quadrilateral. In the case of a single circularly precessing spin wave, all quadrilaterals vanish except one, a square, which precesses at the spin wave frequency in our animated display, implemented in Open Inventor.

In Fig. 3a we show a snapshot of this k-space window at the time labeled "0.30 ns" along the trajectory in Fig. 2. The expected quadrilaterals (discretized ellipses) collapse to lines, indicating linear polarization; the polarization direction rotates with time. The vector from the origin representing $\mathbf{M}(\mathbf{k} = \mathbf{0})$ is shortened by perspective, since it points away from the viewer – it is actually longer than the apparently-longest line (degenerate ellipse) centered at $\mathbf{k} = (2\pi/L, 0, 0)$. The largest mode amplitudes are shown in Fig. 3b. Several of the modes show exponential growth (in principle, straight lines in a log plot) but we expect the lines to have some curvature, because the system started at $t = 0$ at a point where all spin waves are stable (corresponding to oscillations in Fig. 3b) We can see the instability growth rate increase as the magnetization swings toward the hard plane. It can be seen that the three longest-wavelength modes ($k = 2\pi/L$ in the x , y , and z directions) are about equally unstable; which one dominates depends on the random initial condition. Work is ongoing on the effects of boundaries and magnetostatic interactions on this mechanism.

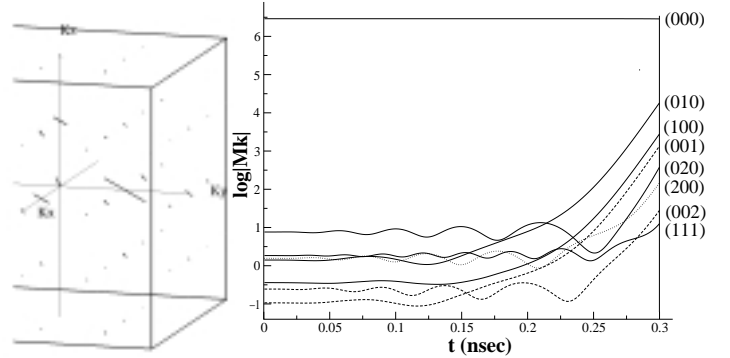


FIG. 3. (a) Snapshot of the k-space window showing the spin wave amplitudes at $t=0.300$ ns. Relative to each k-point, the vector positions of the corners of the quadrilateral are the values of terms in Eq.5. Because of $\mathbf{k} \leftrightarrow -\mathbf{k}$ symmetry, only points with $k_y > 0$ are shown. Movie showing complete evolution is available at <http://bama.ua.edu/~visscher/mumag/switch1.mov>. (b) Logarithmic plot of growth of spin wave. Vertical line at right indicates the time of the snapshot in part (a).

IV. SUMMARY

We have developed a method for spin-wave visualization that allows the understanding of a mechanism of spin-wave switching. This visualization scheme should also be useful for standing waves in finite rectangular solids such as MRAM elements, which can be studied using Brillouin scattering¹⁰.

V. ACKNOWLEDGEMENTS

This work was partially supported by DOE grant No. DE-FG02-98ER45714 and NSF grant DMR-9809423, and by the Computational Materials Sciences Network sponsored by the Materials Sciences Division of the DOE Office of Science.

-
- ¹ J. D. Hannay, R. W. Chantrell, and H. J. Richter, "Simulations of fast switching in exchange coupled longitudinal thin-film media", *J. Appl. Phys.* **85**, 5012 (1999).
 - ² H. Fang and J. G. Zhu, "Switching Speed of Longitudinal Thin Film Recording Media", *IEEE Trans. Mag.* **32**, 3584-3586 (1996).
 - ³ T. J. Silva, C. S. Lee, T. M. Crawford, and C. T. Rogers, "Inductive measurement of ultrafast magnetization dynamics in thin-film Permalloy", *J. Appl. Phys.* **85**, 7849-7862 (1999).
 - ⁴ L. He, W. D. Doyle, and H. Fujiwara, "High Speed Switching in Magnetic Recording Media", *J. Magn. Magn. Mat.*, **155**, 6-12 (1996).

- ⁵ A. Aharoni, "Introduction to the Theory of Ferromagnetism", Oxford U. P., 1996.
- ⁶ V. L. Safonov and H. N. Bertram, *J. Appl. Phys.* **85**, 5072 (1999).
- ⁷ J. Fidler and T. Schrefl, *J. Phys. D* **33**, R153 (2000).
- ⁸ R. W. Chantrell, J. D. Hannay, M. Wongsam, T. Schrefl, and H. J. Richter, *IEEE Trans. Mag.* **34**, 1839 (1998).
- ⁹ Xuebing Feng and P. B. Visscher, "Coarse-graining Landau-Lifshitz damping", *Journal of Applied Physics*, **89**, 6988, 2001.
- ¹⁰ J. J. Jorzick, S.O. Demokritov, B. Hillebrands, "Spin wave quantization in laterally confined magnetic structures" (review), *J. Appl. Phys.* **89**, 7091 (2001).